High-fidelity Imaging Response Detection in Multiple Sclerosis

Dr Baris Kanber,
Translational Imaging Group,
Centre for Medical Image Computing,
Department of Medical Physics and Biomedical Engineering,
University College London

Background

- It is very important to be able to detect an imaging response to treatment in MS as imaging response often occurs before clinical response becomes material.
- However, bulk imaging measures such as the total lesion volume, the number of lesions, and brain parenchyma volume provide limited sensitivity for detecting an imaging response to treatment in MS.
  - i.e. they are too reductive.
- We hypothesised that automated, high-dimensional analysis of clinical MRI can sensitively capture the imaging effect of an intervention.

Approach

- Partition a collection of longitudinal scans in patients treated with natalizumab into sets that are either before or after the treatment boundary.

- Attempt to detect the treatment effect based on low- and high-dimensional models of trajectories of change.

Trajectories of Change

Treatment boundary

Scan 1 Scan 2 Scan 3

Total lesion volume +ve
Total brain volume -ve
Total brain disconnectome +ve
Number of lesions +ve
.
.
High-dimensional versions of the above

Scan 4 Scan 5

Total lesion volume -ve
Total brain volume +ve
Total brain disconnectome -ve
Number of lesions No change
.
.
High-dimensional versions of the above

Models

- Low dimensional:
  - Total lesion volume
  - Number of lesions
  - Total brain volume
  - Total brain disconnectome
  - Age and gender
- High dimensional:
  - Regional brain volumes
  - Regional brain disconnectome map
  - Best features from the above two

Brain Parcellation and Lesion Segmentation

T1-weighted structural scan

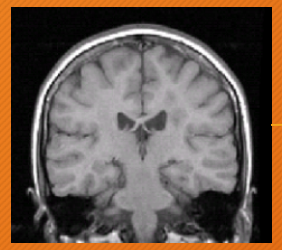

T2-FLAIR

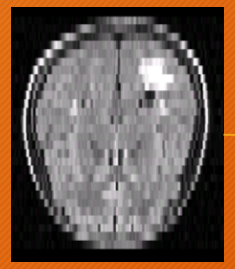

Brain Parcellation

(Cardoso et al., IEEE Trans Med Imaging, 2015)

Level 1 segmentation

(Prados et al. ISBI Longitudinal MS Lesion Segmentation Challange, 2015)

Final segmentation

(Sudre et al. IEEE Trans Med Imaging, 2015)

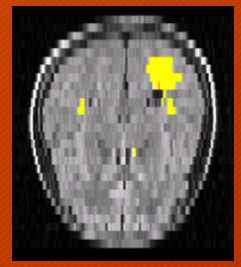

Disconnectome

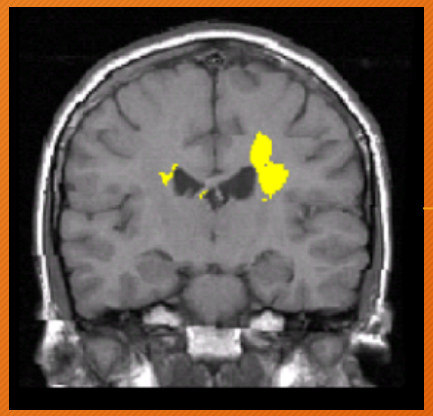

Lesion mask

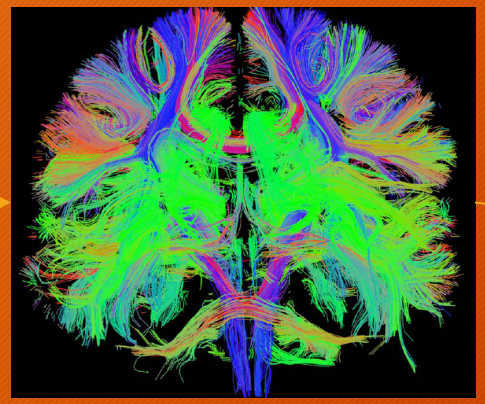

Tractography from healthy subjects

"Brain, Connectivity, Behaviour" Toolkit

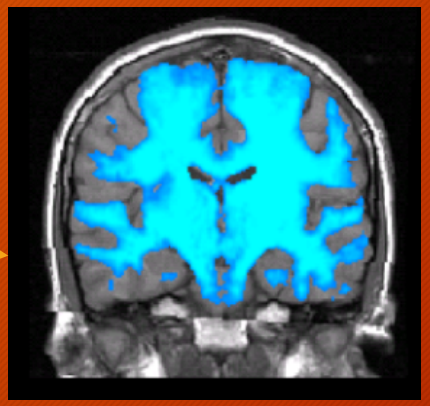

Disconnectome map

Tractography image from: http://www.nrronline.org

Inferential technique

- Classifiers:
  - Support vector machines (rbf kernel).
  - Extremely randomised decision trees (Tree-splitting metric: gini impurity).
- Bootstrapped cross-validation with fully held out test sets

Dataset

- 125 patients with remitting, relapsing MS
  - Data acquired over 15 years
  - 80 female, 45 male
  - Age at the start of treatment: mean: 38, range: 18-70
  - 166 pre-treatment, 413 post-treatment scans
  - T1-weighted structural, and T2-FLAIR scans included

Methods

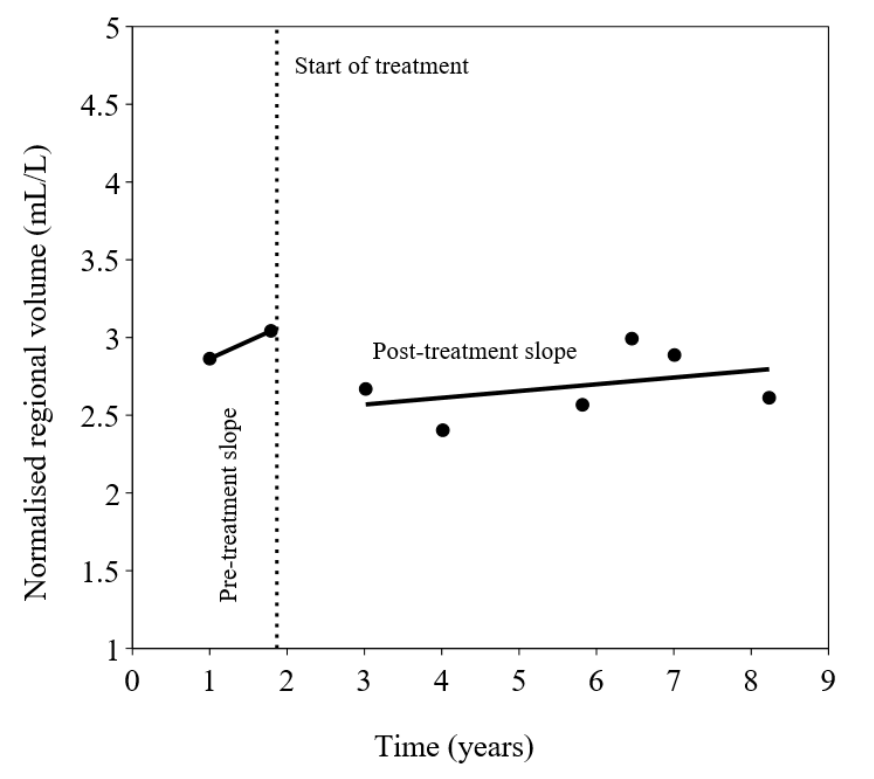

Figure above for the thalamus (right hemisphere) in a single patient.

- Adjusted for:
  - Age, gender, scanner manufacturer, field strength, T1 voxel size, FLAIR voxel size, disease duration, and EDSS.
  - …using residuals from Bayesian Penalised Regression Estimation.

Results

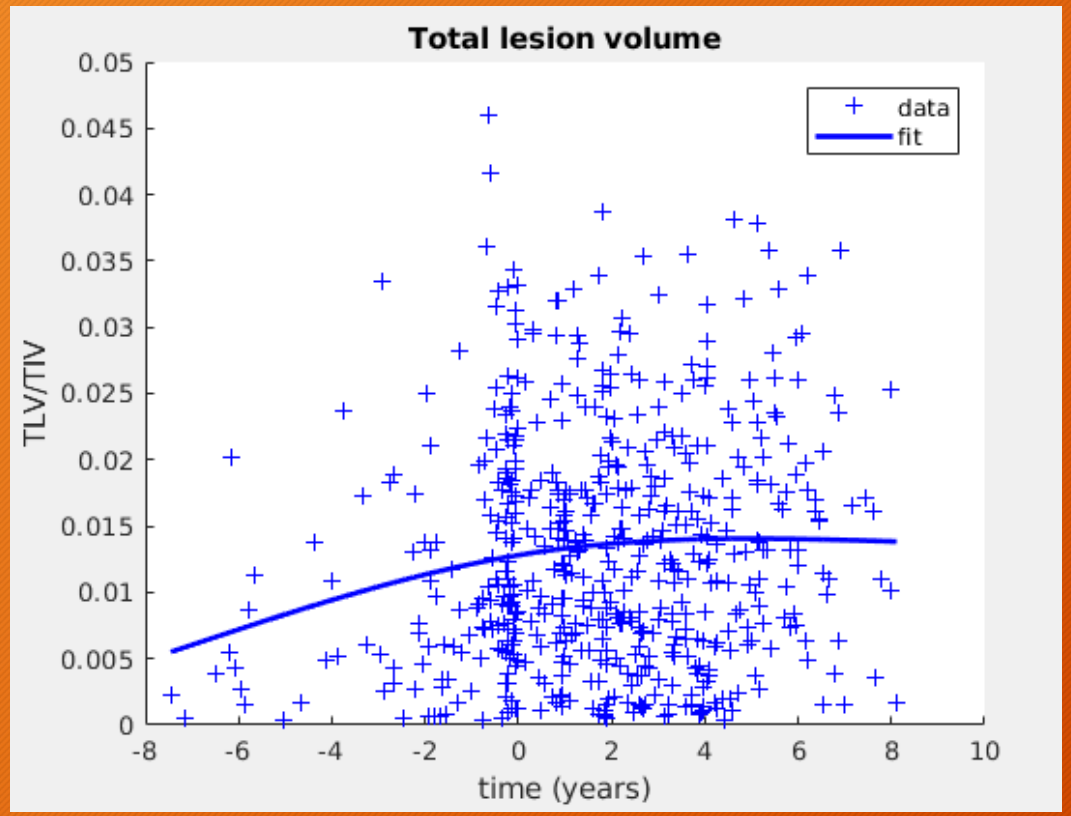

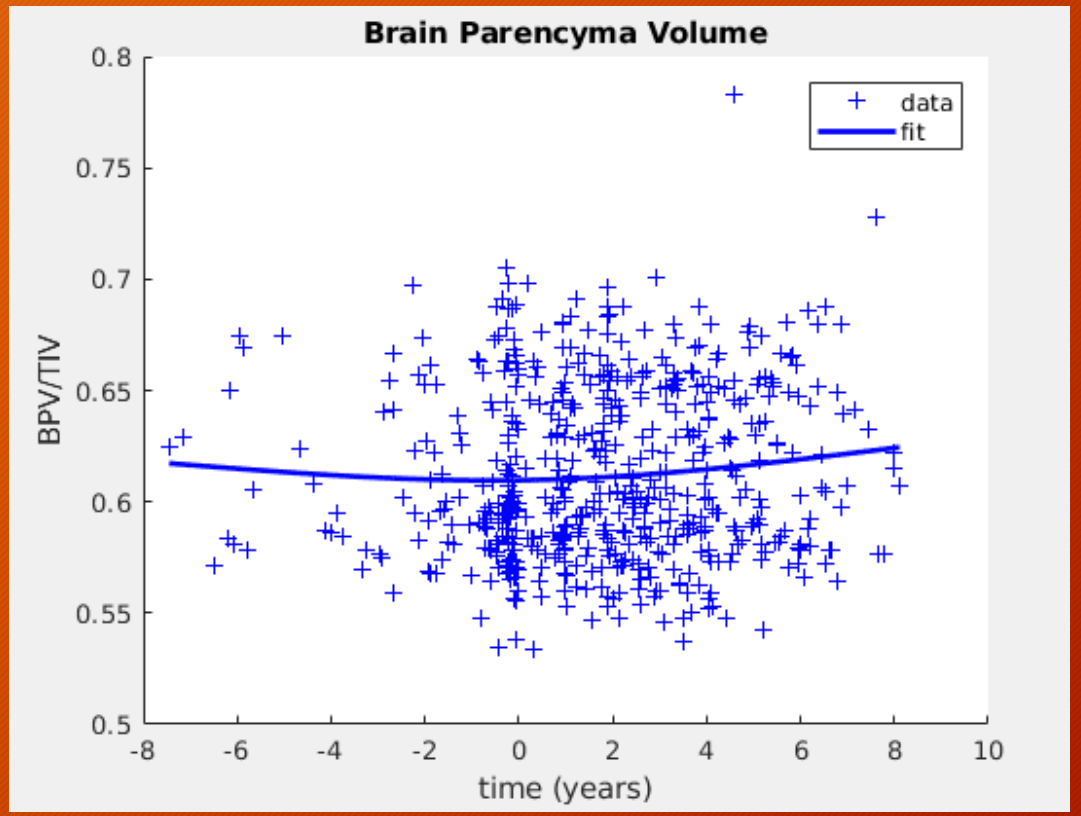

Fitted lines are obtained with Restricted Cubic Spline Regression

Total lesion volume

Pre-treatment Post-treatment

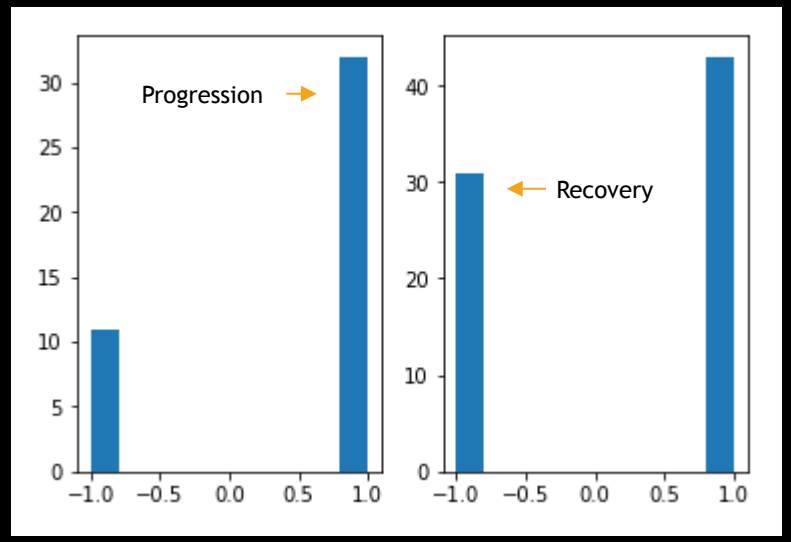

Total brain disconnectome

Pre-treatment Post-treatment

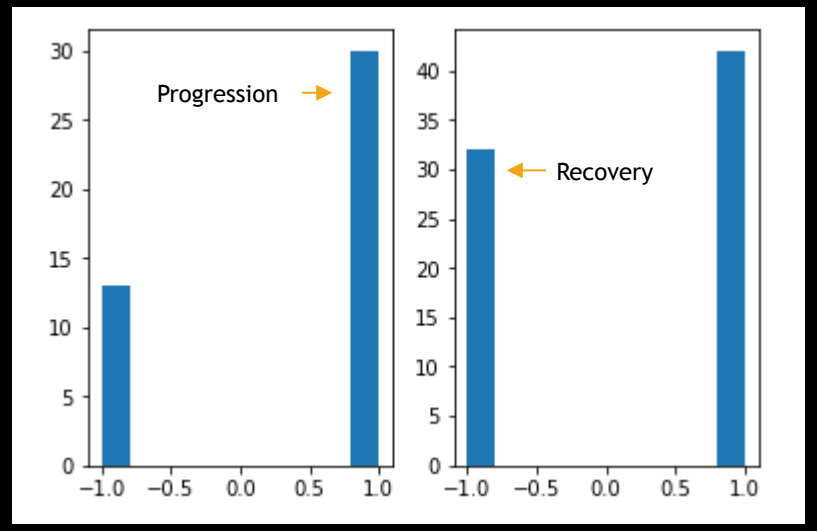

Group-level histograms of trajectories for the low-dimensional biomarkers.

Number of lesions

Pre-treatment Post-treatment

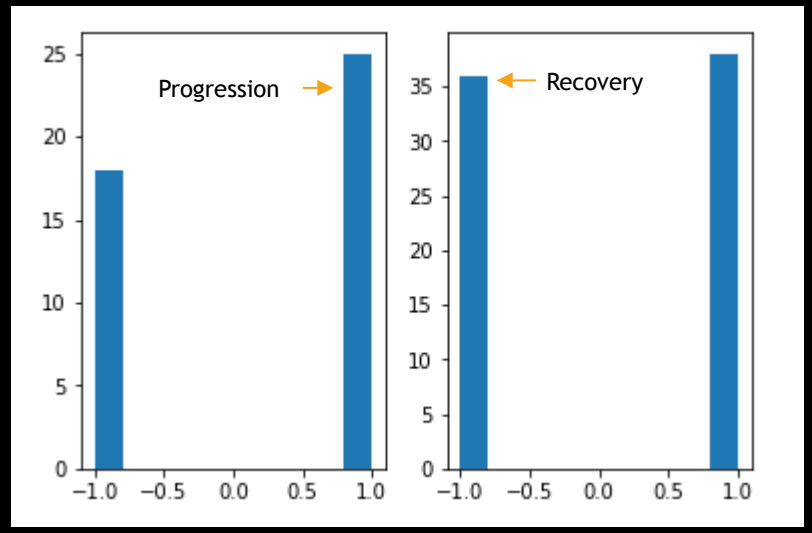

Brain parenchyma volume

Pre-treatment Post-treatment

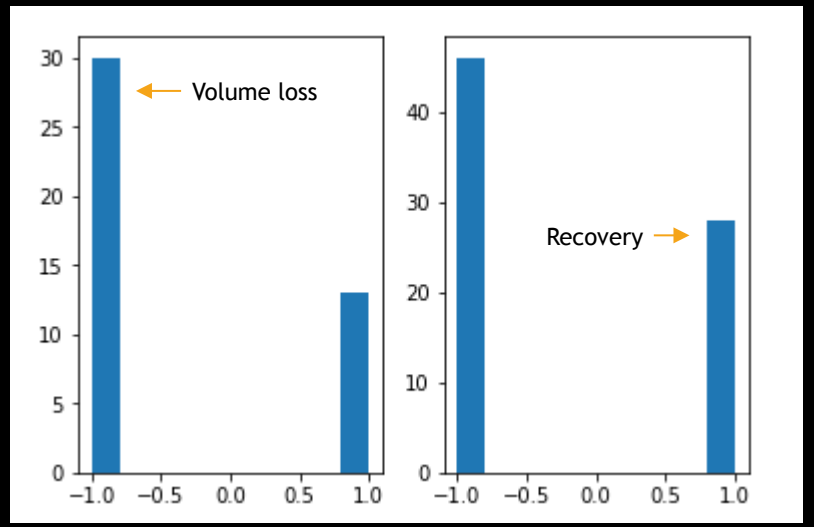

High-dimensional biomarkers are the equivalents of these for the various regions of the brain as opposed to the brain as a whole.

Results

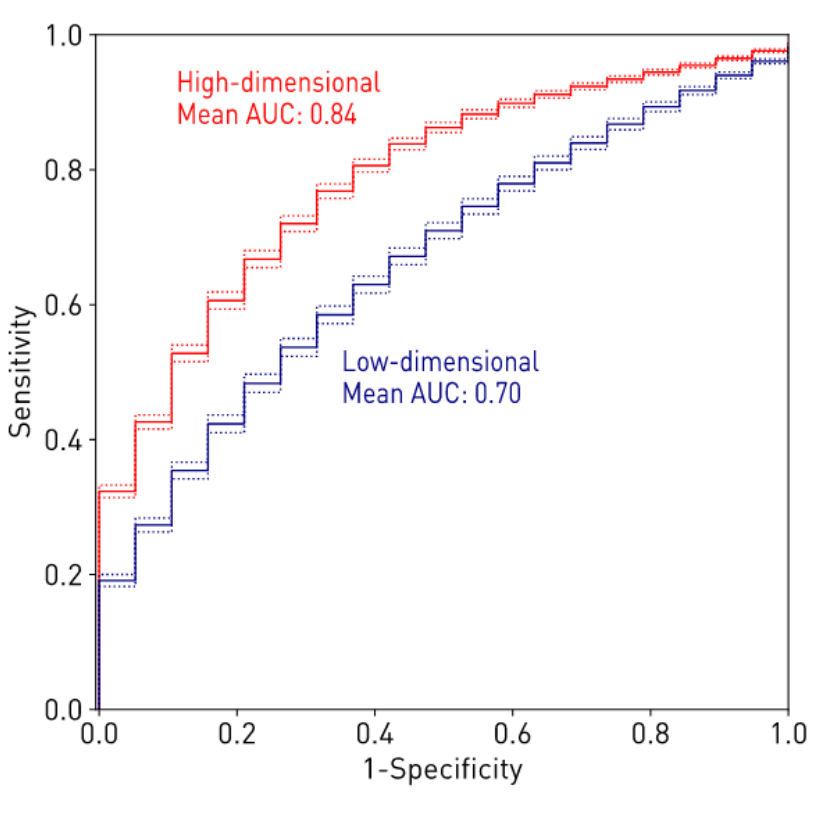

- Both the low and high-dimensional models could predict the imaging response to treatment: both ROC curves of both differed significantly from chance (P<0.01 for both).
- However, there was also a significant statistical difference between the ROC curves of the high- and low-dimensional models (P<0.01).
- The best high-dimensional model yielded a mean area under the ROC curve of 0.843 (95% CI: 0.835-0.851) which was significantly higher than 0.700 (95% CI: 0.691-0.709) obtained with the best low-dimensional model (P<0.01).

** Two-sided, two-sample Kolmogorov-Smirnov tests.

Results

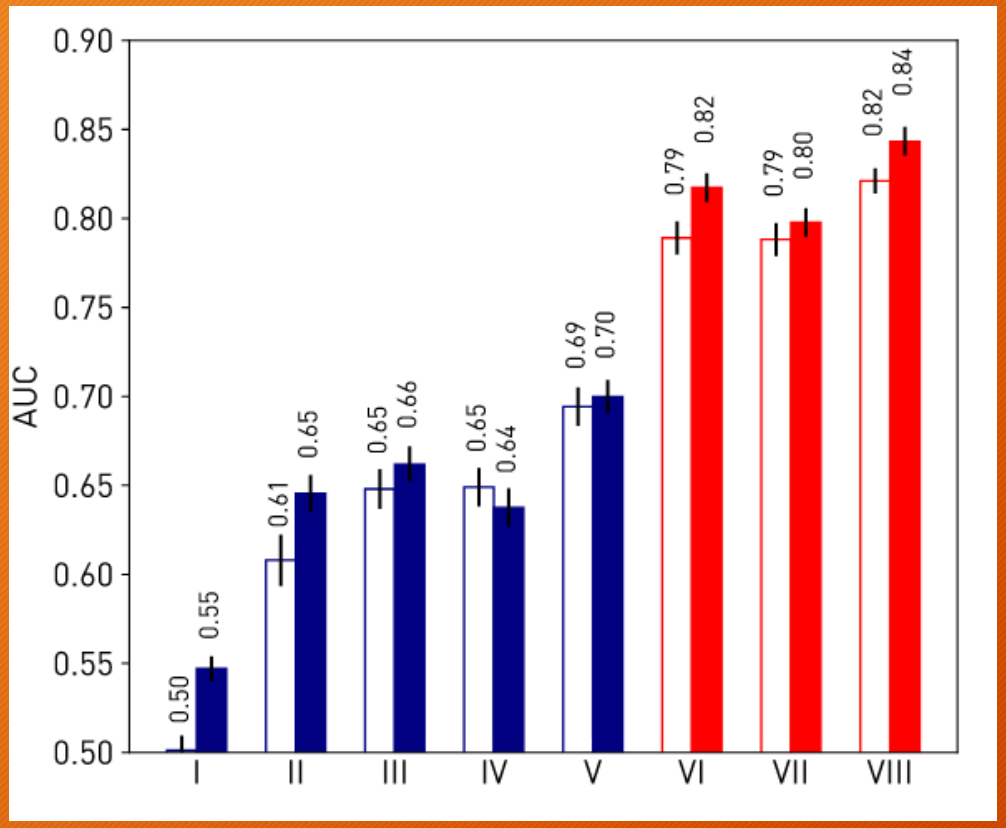

- Figure left:
  - Models are drawn in *blue* for the low-dimensional and *red* for the high-dimensional and are:
    - **I** (age and gender)
    - **II** (the number of lesions)
    - **III** (the total lesion volume)
    - **IV** (brain volume)
    - **V** (best low-dimensional)
    - **VI** (regional brain volume trajectories)
    - **VII** (regional disconnectome trajectories)
    - **VII** (best high-dimensional).
  - Classifiers are: SVM (*unfilled bars*), and ERT (*filled bars*).

- Although the ERT classifier outperformed SVM for the best models, the superior performance of the high-dimensional models was consistent for both classifiers.

Results

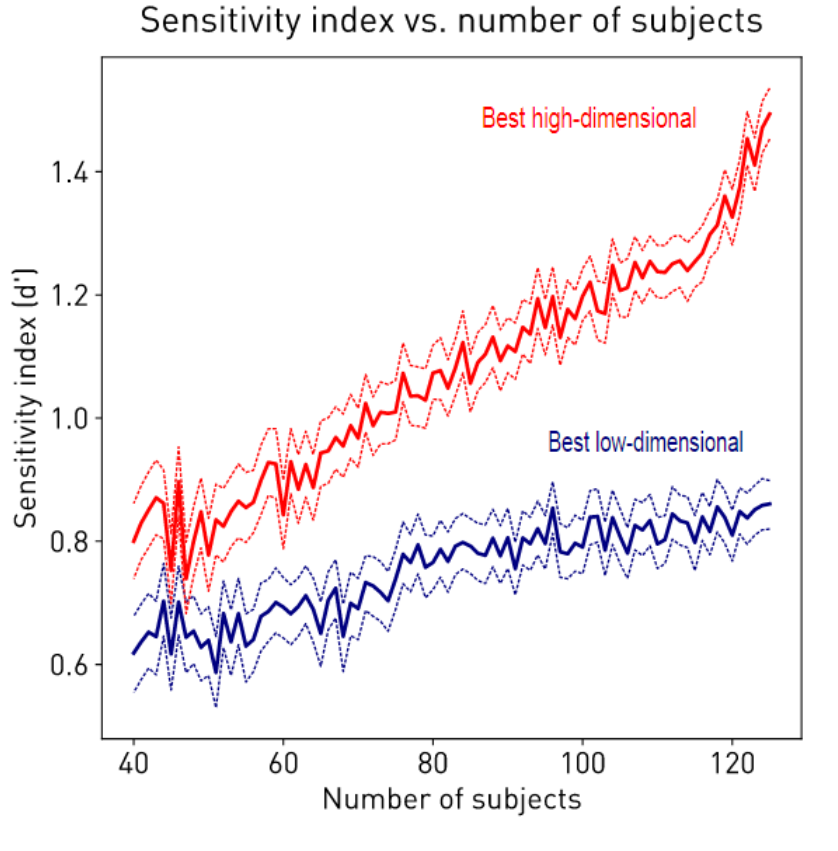

- Performance of the best high-dimensional model surpassed that of the best low-dimensional model across the entire range.
  - Performance disparity increased with the number of patients.
  - No evidence that a plateau had been reached.

- Limited gains in increasing the number of subjects if you remain low-dimensional.

Results

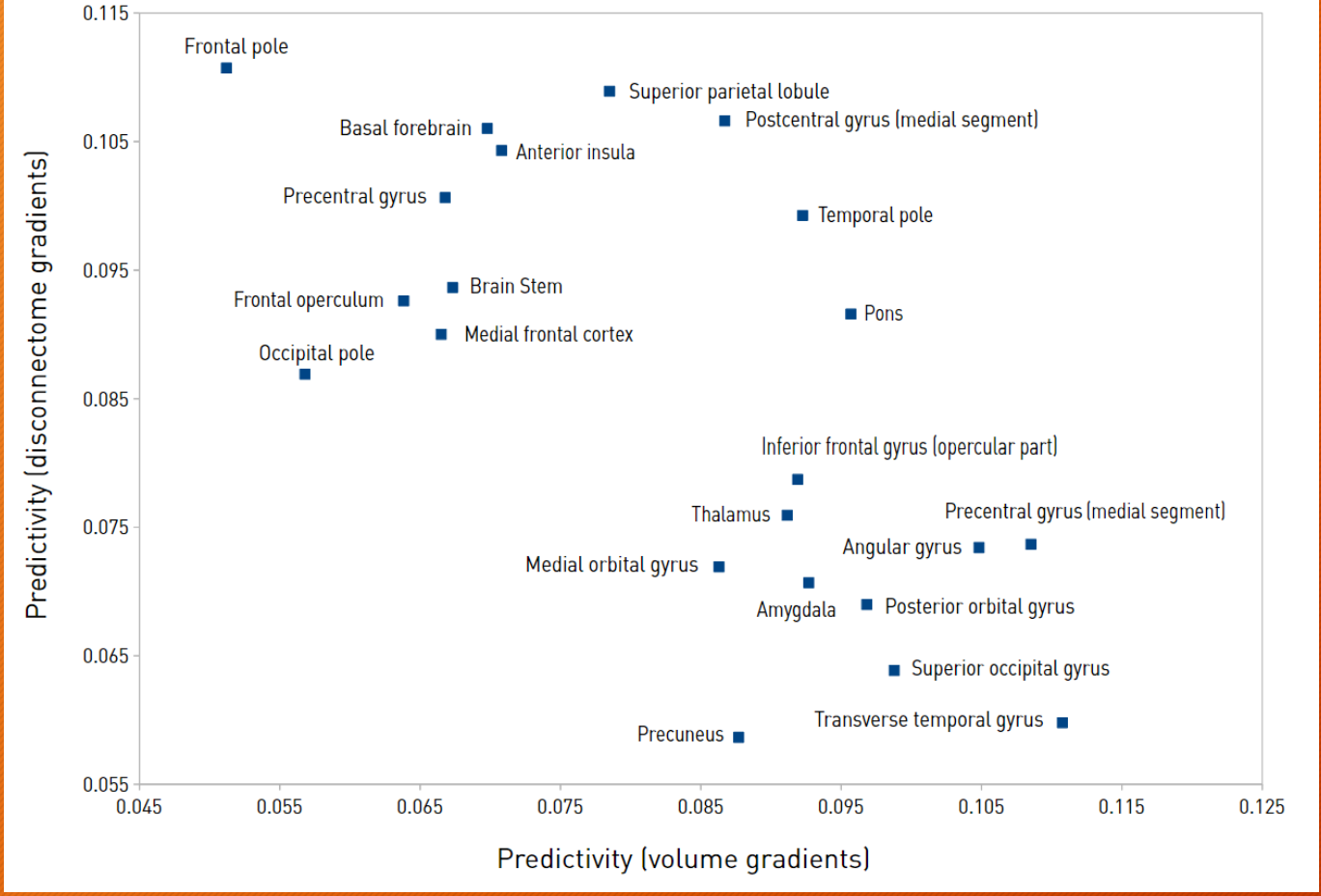

- Relative predictivities of the disconnectome trajectories vs. relative predictivities of the volume trajectories for the brain regions most influential for imaging response detection.
  - Predictivities for each highly ranking brain region are in arbitrary units.

- The imaging features most relied upon by the best high-dimensional classifier were consistent with known patterns of lesion and parenchymal change in multiple sclerosis.

Conclusion

- Therapeutic effects can be sensitively detected by high-dimensional analysis of clinical neuroimaging.
- If it works for clinical imaging it is going to be even better for research imaging.
- We can monitor post-market much more sensitively than we currently do.

References

Rojkova et al.	Atlasing the frontal lobe connections and their variability due to age and education: a spherical deconvolution tractography study.	Brain Struct Funct.	2016	221(3)	1751-66
Thiebaut de Schotten et al.	A lateralized brain network for visuospatial attention.	Nat Neurosci.	2011	14(10)	1245-6
Klein et al.	Evaluation of 14 nonlinear deformation algorithms applied to human brain MRI registration.	Neuroimage	2009	46(3)	786-802
Avants et al.	A reproducible evaluation of ANTs similarity metric performance in brain image registration.	Neuroimage	2011	54(3)	2033-44
Wang et al.	Diffusion Toolkit: A Software Package for Diffusion Imaging Data Processing and Tractography	Proc. Intl. Soc. Mag. Reson. Med.	2007		3720
Thiebaut de Schotten et al.	Atlasing location, asymmetry and inter-subject variability of white matter tracts in the human brain with MR diffusion tractography.	Neuroimage	2011	54(1)	49-59
Thiebaut de Schotten et al.	From Phineas Gage and Monsieur Leborgne to H.M.: Revisiting Disconnection Syndromes.	Cereb Cortex	2015	25(12)	4812-27
Oliphant T.E.	A Bayesian perspective on estimating mean, variance, and standard-deviation from data	http://scholarsarchive.byu.edu/facpub/278	2006		
Geurts et al.	Extremely randomized trees	Mach Learn	2006	63(1)	3-42
Chang and Lin	LIBSVM : a library for support vector machines.	ACM Transactions on Intelligent Systems and Technology	2011	2	1-27
Pedregosa et al.	Scikit-learn: Machine Learning in Python	JMLR	2011	12	2825-2830
Modat et al.	Fast free-form deformation using graphics processing units	Computer methods and programs in biomedicine	2009	98(3)	2009
Kanber et al.	An integrated imaging informatics software platform to improve the analysis of clinical trials and research data in MS	ECTRIMS	2016		